UDC 551.515.21:551.509.313

NUMERICAL EXPERIMENTS WITH A SLOWLY VARYING MODEL OF THE TROPICAL CYCLONE

RICHARD A. ANTHES

National Hurricane Research Laboratory, Environmental Research Laboratories, NOAA, Miami, Fla.

ABSTRACT

Additional experiments with the slowly varying axisymmetric hurricane model described by Anthes are presented. Variable horizontal eddy viscosity coefficients are utilized to study circulations that result from an increased heating function and a heating function with a double maximum along the radial direction. Infrared radiative cooling is modeled for the clear tropical atmosphere following Sasamori. A representative cooling rate is used to study the effect of cooling in the hurricane environment on the dynamics and energetics of the slowly varying tropical cyclone.

1. INTRODUCTION

Preliminary results from a steady-state axisymmetric tropical cyclone model in isentropic coordinates have been presented in detail in paper I, a companion paper (Anthes 1971). These experiments showed that slowly varying states of the mass and momentum fields which were representative of tropical cyclones could be obtained as a direct result of steady thermal forcing. The experiments in paper I established values for horizontal and vertical momentum exchange coefficients, horizontal resolution, and domain size that yield realistic results for this model. The energetics of the slowly varying states were emphasized.

This paper (II) briefly summarizes the results of later experiments investigating additional heating distributions and a variable horizontal eddy viscosity coefficient. In particular, the latent heating function is increased to generate a more intense hurricane. A horizontal heating distribution with a double maximum is studied to simulate the effect of rainbands. Finally, cooling in the hurricane environment due to longwave radiation is modeled following Sasamori (1968); and the effect of cooling on the dynamics and energetics of the slowly varying hurricane is investigated.

2. SUMMARY OF THE MODEL

The numerical aspects of the steady-state model are summarized in this section for convenience. The model is axisymmetric and consists of six isentropic levels and the sea-level surface. Given arbitrary initial conditions, the mass and momentum fields are "forecast" for a steady heating function utilizing the Matsuno (1966) time integration scheme and centered space differences. The steady heating function is prescribed by assuming a horizontal profile of rainfall rates and distributing the equivalent latent heat vertically. Surface stress is parameterized using a constant drag coefficient of 0.003. Diffusion of momentum and heat is parameterized by constant horizontal exchange coefficients and a vertical eddy viscosity coefficient that decreases linearly upward. The forecast iterations continue until the mass and momentum fields reach a slowly varying state.

3. VARIABLE HORIZONTAL MIXING COEFFICIENTS

Although constant horizontal exchange coefficients for momentum and temperature were used in the previous experiments, the physical basis for the form and value of exchange coefficients is quite uncertain. Other numerical models contain a variable amount of horizontal diffusion, either through the use of exchange coefficients that are functions of the circulation or through horizontal truncation error which also yields a variable diffusion (pseudo-viscosity). The eddy viscosity coefficients of Smagorinsky et al. (1965) and Leith (1969) which are proportional to the local deformation of the velocity field and gradient of vorticity, respectively, belong to the first category. Orville's (1968) cloud model and Rosenthal's (1970) hurricane model which employ upstream differencing in the advection terms are examples belonging to the second category. Comparison of the relative merits of the various parameterizations is difficult and seems mainly to be a subjective judgment on which gives best results for the particular model.

Symbols used frequently in this work are:

c_p	specific heat at constant pressure,
g	acceleration of gravity,
K_H	horizontal coefficient of eddy viscosity,
p	pressure,
q	water vapor mixing ratio,
r	radial distance,
Δr	horizontal grid increment,
$R(u, T)$	absorptivity,
T	absolute temperature,
u	path length,
z	height,
Δz	vertical grid increment,
θ	potential temperature,
ρ	air density, and
σ	Stefan-Boltzmann constant $=8.13\times10^{-11}$ cal $\cdot$ cm$^{-2}\cdot$ cm°K$^{-4}\cdot$ min^{-1}.

For comparing the effects of variable and constant horizontal diffusion coefficients in this model, the experiments in sections 3 and 4 are computed following

Smagorinsky et al. (1965) in which the exchange coefficient for momentum is proportional to the local deformation. For cylindrical coordinates and circular symmetry, the expression for K_H is

$$K_H=k_0^2\Delta r^2|D| \tag{1}$$

where the deformation, D, is

$$|D|=r\left\{\left[\frac{\partial}{\partial r}\left(\frac{v_r}{r}\right)\right]^2+\left[\frac{\partial}{\partial r}\left(\frac{v_\lambda}{r}\right)\right]^2\right\}^{1/2}. \tag{2}$$

The nondimensional parameter, k_0, is the Kármán constant. Smagorinsky et al. (1965) found that a value of k_0 equal to 0.4 gave the best results in a general circulation model. In some trial experiments with the hurricane model, this value gave somewhat overdamped solutions; therefore, a value of 0.28 was selected for the following experiments.

The experiments in sections 3 and 4 utilize a domain size of 500 km and a variable grid with 10-km resolution from the origin to 200 km decreasing gradually to 25 km at the edge of the domain. This grid was shown to be an accurate substitution for a high-resolution constant grid in paper I. The time step is 15 s, and all results correspond to 3,200 iteration steps.

A. UPPER LEVEL PRESSURE SURFACE OF 140 MILLIBARS, EXPERIMENT 1

For establishing continuity with previous experiments, experiment 1 utilizes the same heating function used in most of the experiments in paper I (see also rainfall type A in fig. 1 of paper II). The slowly varying momentum profiles for experiment 1 are shown in figure 2. The results using the variable coefficients are most similar to those with a constant coefficient, K_H, of 2.5×10^8 cm^2/s. The variable coefficient yields less mixing, however, as shown by an increase in maximum tangential wind from 41 in experiment 14 of paper I to 48 m/s. The energy budget, summarized in table 1, also shows a decrease in horizontal dissipation of kinetic energy. For the variable coefficient, the ratio of lateral dissipation to total dissipation is about 1/20; whereas for a constant coefficient of 2.5×10^8 cm^2/s, the ratio is about 3/20.

B. UPPER LEVEL PRESSURE SURFACE OF 110 MILLIBARS, EXPERIMENT 2

The experiments in which moderate storms are generated by a heating function maximum of 50 cm of rain per day have utilized the upper boundary condition of pressure equal to 140 mb. For intense storms, however, the undisturbed level occurs at a lower pressure (Koteswaram 1967). Therefore, in preparation for an increased heating

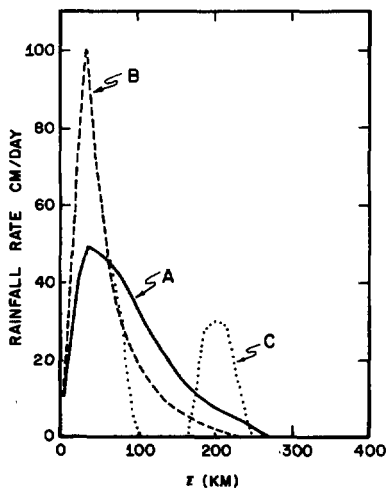

FIGURE 1.—Radial profiles of rainfall rates used to specify horizontal variations of the latent heating function.

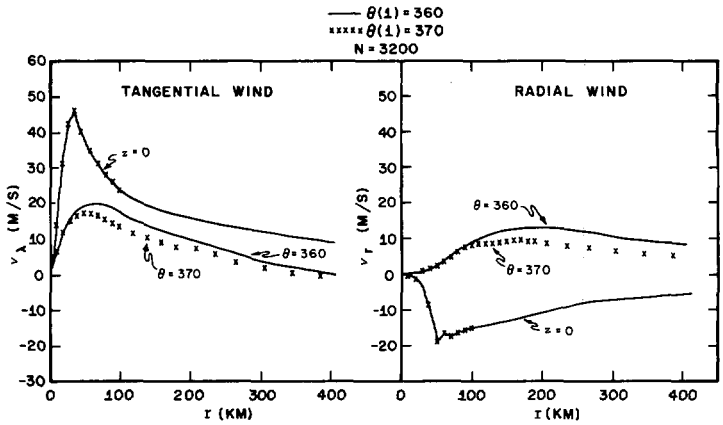

FIGURE 2.—Tangential and radial wind profiles for experiments 1 and 2.

TABLE 1.—*Summary of experiments*

Exp. no.	Rainfall type	k_0	Central pressure	Max. wind speed	Total heating	G(A)	B(A)	C(A)	Drag dissipation	Lateral mixing	Vertical mixing
			(mb)	(m/s)	(10^{14} W)	(10^{12} W)	(10^{12} W)	(10^{12} W)	(10^{12} W)	(10^{12} W)	(10^{12} W)
1	A	0.28	970.1	52	11.2	8.0	4.2	14.8	−9.0	−1.0	−11.6
2	A	0.28	970.8	51	11.8	6.5	2.6	10.8	−8.9	−1.0	− 9.6
3	A	0	963.8	61	11.8	5.9	2.5	10.2	−9.3	0	− 9.6
4	B	0.28	962.6	55	8.7	6.7	1.1	9.7	−8.7	−1.7	− 7.9
5	C	0.28	974.6	48	11.2	3.9	2.0	7.4	−7.8	−1.0	− 7.0
6	A	$K_H=5\times10^8$ cm^2/s (constant)	984.9	38	7.6	14.6	2.4	19.0	−9.4	−5.9	−13.0

G(A) generation of available energy
B(A) boundary available energy
C(A) conversion of available energy to kinetic energy

TABLE 2.—*Old and new isentropic levels and approximate mean pressures (Jordan 1958)*

Level	Old		New	
	θ (°K)	p (mb)	θ (°K)	p (mb)
1	360	140	370	110
2	350	190	360	150
3	340	300	350	190
4	330	440	335	370
5	320	580	320	580
6	310	760	310	760

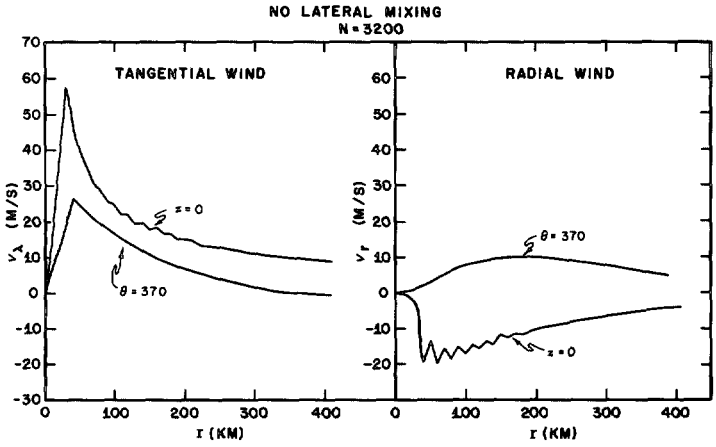

FIGURE 3.—Tangential and radial wind profiles for experiment 3.

function, experiment 1 is repeated with an upper boundary of 110 mb. The information levels are redefined so that the number (6) of isentropic levels remains the same (table 2).

The slowly varying solutions for experiment 2 with the higher upper surface are quite similar to those in experiment 1 (fig. 2). Although the low-level profiles are virtually identical, the upper levels show somewhat weaker outflow in experiment 2. This difference is probably related to the deeper outflow layer in experiment 2.

C. NO LATERAL DIFFUSION OF MOMENTUM, EXPERIMENT 3

All experiments with the steady-state hurricane model have contained some form of horizontal momentum diffusion. It is interesting, however, to run one experiment with no horizontal diffusion whatsoever, ($K_H=0$). Because of the nonlinear terms in the equations of motion, difficulty may be expected from the accumulation of energy in the short wavelengths that may lead to nonlinear instability (Phillips 1959).

Figure 3 shows the momentum profiles for experiment 3 that contains no horizontal diffusion of momentum. In contrast to the smooth profiles of previous experiments, standing space oscillations of wavelength $2\Delta r$ appear in the low-level profiles where horizontal advection is greatest. These oscillations do not amplify with time, but they remain as part of the slowly varying solutions to the finite-difference equations. The nonamplification is apparently related to the steady heating function, the vertical mixing, and the high (time) frequency damping property of the Matsuno integration scheme. The increase in maximum wind speed from 51 to 61 m/s illustrates the sensitivity of the maximum wind to horizontal mixing.

Experiments 1, 2, and 3 have been discussed very briefly to establish continuity with the experiments in paper I. The experiments in section 4 utilize the variable horizontal mixing formulation defined by $k_0=0.28$ and the upper boundary condition of $p=110$ mb.

4. HORIZONTAL VARIATION OF LATENT HEATING

The experiments in paper I considered latent heating functions defined by a single maximum in the rainfall rate profile of 50 cm/day. The strongest maximum wind speed produced by this heating function was only 44 m/s, typical of a weak hurricane. However, empirical (Riehl and Malkus 1961) and numerical (Rosenthal 1970) results indicate that rainfall rates near the center of the hurricane may be substantially greater than 50 cm/day. The first experiment in this section is computed with a rainfall maximum of 100 cm/day in an attempt to generate a stronger vortex. The second experiment considers a heating function with a secondary maximum about 200 km from the storm center, an attempt to investigate the cumulative effect of rainbands on the hurricane circulation.

A. RAINFALL MAXIMUM OF 100 CENTIMETERS PER DAY, EXPERIMENT 4

The experiments in paper I showed that, for given horizontal and vertical exchange coefficients, the maximum winds are determined primarily by the heat release within 100 km. The circulations generated by the heating functions associated with the 50 cm/day rainfall maximum correspond to a weak hurricane; however, the total heating is somewhat higher than empirical evidence. In experiment 4, therefore, the heating maximum at 45 km in experiment 2 is doubled while the heating beyond 100 km is substantially reduced (rainfall type B in fig. 1). The total heating is reduced from 11.8 to 8.7×10^{14} W. All other parameters are identical to those in experiment 2.

The momentum profiles (fig. 4) show an increase in maximum wind speed from 51 to 55 m/s, despite the reduction in total heating. The central pressure drops from 970.8 to 962.6 mb. The circulation at larger radii is slightly less, as indicated by the small reduction in outflow at 400 km and in the various components of the energy budget (table 1). The features of the circulation and the components of the energy budget for experiment 4 correspond to a moderate hurricane.

The results from experiment 4 with the increased heating maximum confirm that the maximum wind is determined primarily by the heat release inside 100 km

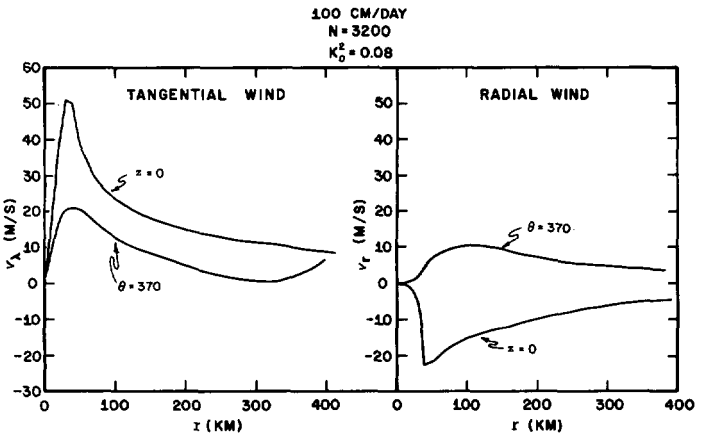

FIGURE 4.—Tangential and radial wind profiles for experiment 4.

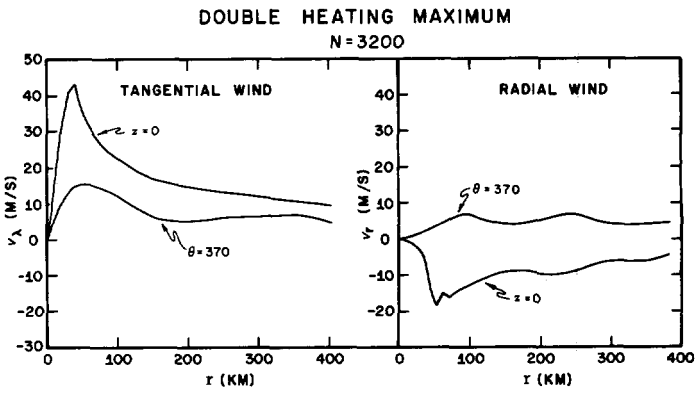

FIGURE 5.—Tangential and radial wind profiles for experiment 5.

and that variations in heating in the outer regions affect mainly the horizontal extent of the storm circulation.

B. SECONDARY HEATING MAXIMUM AT 200 KILOMETERS, EXPERIMENT 5

In the final experiment with the horizontal variation of heating, a secondary heating maximum is introduced at 200 km (rainfall type C in fig. 1). The introduction of a secondary heating maximum is an attempt to investigate the possible role of hurricane rainbands in which substantial precipitation occurs at some distance from the center (Gentry 1964). Although rainbands are generally asymmetric, the mean effect in an axisymmetric model appears as a ring of enhanced convection.

The results from experiment 5 show rather small changes from those in experiment 2. The secondary heating maximum reduces the maximum wind from 51 to 48 m/s and raises the central pressure 4 mb (fig. 5 and table 1). The radial wind profile shows a weaker circulation inside 200 km, and the single outflow maximum in experiment 2 is replaced by two weaker maxima in experiment 5. The rather small differences in the circulations inside 100 km again emphasize the insensitivity of the maximum wind to changes in heating at large (200 km) distances from the center in the steady-state model.

Experiment 5 may have some relevance to hurricane modification experiments (*PROJECT STORMFURY, Annual Report*, Staff, National Hurricane Research Laboratory 1969). One aspect of Project STORMFURY involves seeding supercooled water in rainbands with silver iodide crystals. The additional heat of fusion might then stimulate additional convective heating at this distance and possibly reduce the amount of air reaching the center by deviating the inflow upward. This chain of events would then result in a decrease of the maximum winds near the center.

The changes in circulation in experiment 5 that result from an increase in heating at 200 km are small but qualitatively confirm the hypothesis of the rainband experiments in Project STORMFURY. However, the results are inconclusive. From one point of view, it may be argued that the reduction in maximum winds is small in comparison to the changes in the heating distribution. On the other hand, if the hurricane vortex is unstable, a small change might produce interactions that cause greater differences with time. The steady-state model, of course, is not capable of studying such feedback.

The two experiments in section 4 have shown that a heating maximum defined by a rainfall rate of 100 cm/day is adequate to drive a moderate hurricane and indicate that the presence of a secondary heating maximum away from the storm center has a relatively small effect on the maximum wind near the center. Both experiments confirm the primary dependence of the maximum wind on the heat release inside 100 km. Section 5 shows the investigation of the role of infrared cooling on the steady-state hurricane.

5. INFRARED RADIATIVE COOLING IN THE HURRICANE ENVIRONMENT

Because of the immense importance of latent and sensible heat as energy sources in the tropical cyclone system, little attention has been directed toward infrared cooling as a sink of energy. In numerical experiments to date, only Ooyama (1969) included the effect of radiative cooling. Ooyama experimented with a uniform cooling rate and found little change from the noncooling cases. He notes, however, that differential cooling may affect the development of tropical cyclones.

In a study of hurricane Hilda, 1964, Anthes and Johnson (1968) estimated that infrared cooling in the outer region of the storm could account for 15 to 20 percent of the total generation of available potential energy on the hurricane scale (1000 km). The total cooling nearly equaled the total latent heating on this scale. It is important, therefore, to ascertain whether radiative cooling represents a passive energy loss or contributes actively toward maintaining the baroclinicity in the hurricane.

If the 15- to 20-percent generation by infrared emission is representative, the effect of the cooling on the dynamics should be investigated, in view of the strong correlation between generation of available energy and conversion to kinetic energy in these experiments. The next section presents radiative cooling rates in the clear tropical atmosphere, which are computed using Sasamori's (1968) radiation model. Sasamori's model is quite suitable for use in numerical models of the tropical cyclone because of its relative simplicity and computational economy in terms of speed and storage.

Because of the small magnitude of the diabatic cooling by the divergence of infrared radiation and the uncertainties in the heating and mixing parameterization in the isentropic model, the estimation of an infrared cooling profile with high resolution is not required. However, profiles of infrared cooling from several temperature and moisture distributions are presented to illustrate ranges of cooling for various tropical conditions and to justify the use of a mean cooling rate. The basic temperature and moisture distribution is Jordan's (1958) mean hurricane season sounding, which will be considered representative of the nearly cloud-free region surrounding the storm.

A. COMPUTATIONAL PROCEDURE

In Sasamori's (1968) model, the absorptivities for water vapor (H_2O), carbon dioxide (CO_2), and ozone (O_3) that are complicated functions of path length and temperature are approximated by empirical formulas. However, in these experiments where only the troposphere is considered, the effect of ozone is neglected. Sasamori's model is now summarized to study profiles of cooling in the tropical atmosphere.

The net flux of radiation through a unit area is a function of the amount of absorbing gas above and below the layer, as well as the vertical temperature profile. The mean absorptivity, R, is

$$R(u, T)=\int_0^\infty [1-\tau(u)]\frac{dB_\nu}{dT}\,d\nu \tag{3}$$

where B_ν is Planck's radiation function expressed in flux at frequency ν, T is temperature, and τ represents the mean transmissivity. The effective path length, u, is approximately

$$u\approx g^{-1}\int_{p_1}^{p_2} q\left(\frac{p}{p_0}\right)dp \tag{4}$$

with q as the mixing ratio and $p_0=1000$ mb.

At any level, z, the downward and upward fluxes are

$$F\downarrow(z)=\int_0^{T(z)} R\{u(T')-u[T(z)],\ T'\}dT' \tag{5}$$

and

$$F\uparrow(z)=\sigma T_0^4+\int_{T_0}^{T(z)} R\{u[T(z)]-u(T'),\ T'\}dT' \tag{6}$$

with σ equal to the Stefan-Boltzmann constant (8.13×10^{-11} cal·cm^{-2}·°K^{-4}·min^{-1}); T_0, the surface temperature; and T', the variable of integration corresponding to temperature.

The radiative temperature change calculated from the net vertical flux divergence is

$$\frac{\partial T}{\partial t_R}=-\frac{1}{\rho c_p}\frac{d(F\uparrow-F\downarrow)}{dz}. \tag{7}$$

Sasamori transforms $R(u, T)$ to a normalized absorptivity given by

$$\overline{A}(u, T)=\frac{R(u, T)}{4\sigma T^3}=\frac{\int_0^\infty [1-\tau(u)]\frac{dB_\nu}{dT}\,d\nu}{\int_0^\infty \frac{dB_\nu}{dT}\,d\nu}. \tag{8}$$

With this transformation, the downward and upward fluxes are

$$F\downarrow(z)=4\sigma\int_0^{T(z)}\overline{A}\{u(T')-u[T(z)],\ T'\}T'^3dT' \tag{9}$$

and

$$F\uparrow(z)=\sigma T_0^4+4\sigma\int_{T_0}^{T(z)}\overline{A}\{u[T(z)]-u(T'),\ T'\}T'^3dT'. \tag{10}$$

Sasamori notes that the mean absorptivity is nearly constant with temperature in the range +30° to −50°C but decreases with decreasing temperature at extremely low temperatures. For this reason, the integrals in eq (9) and (10) are separated into two parts. For example, eq (9) is written as

$$F\downarrow(z)=4\sigma\int_{T(z_1)}^{T(z)}\overline{A}\{u(T')-u[T(z)],\ T'\}T'^3dT' +4\sigma\int_0^{T(z_1)}\overline{A}\{u[T(z_1)]-u[T(z)],\ T'\}T'^3dT' \tag{11}$$

where z_1 is the height of the level above which the path length changes very little. Disregarding the direct dependency of $\overline{A}(u, T')$ on T' in the first integral and taking $u[T(z_1)]-u[T(z)]$ as constant with T (by definition of z_1) in the second integral, eq (11) becomes

$$F\downarrow(z)=4\sigma\int_{T(z_1)}^{T(z)}\overline{A}_0\{u(T')-u[T(z)]\}T'^3dT' +\sigma T^4(z_1)\overline{\overline{A}}\{u[T(z_1)]-u[T(z)],\ T(z_1)\}. \tag{12}$$

$\overline{A}_0(u)$ is the average absorption for the temperature range +30° to −50°C, and $\overline{\overline{A}}\ (u,T)$ is the mean absorptivity which varies with temperature. $\overline{A}_0(\Delta u)$ and $\overline{\overline{A}}\ (u, T)$, approximated by empirical formulas, are

$$\overline{A}_0(\Delta u)=\begin{cases}0.846(\Delta u+3.59\times10^{-5})^{0.243}-0.069 & \Delta u<0.01\text{ g}\\ 0.240\log_{10}(\Delta u+0.01)+0.622 & 0.01\text{ g}<\Delta u\end{cases} \tag{13}$$

and

$$\overline{\overline{A}}(u, T)=8.34\,T^{[0.353\log_{10}u-0.44]}u^{[-0.03455\log_{10}u-0.705]}. \tag{14}$$

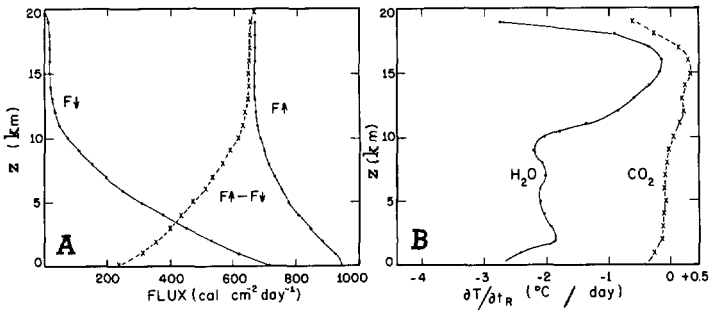

FIGURE 6.—(A) upward, downward, and net infrared flux for the mean tropical sounding and (B) rates of temperature change due to the infrared flux divergence.

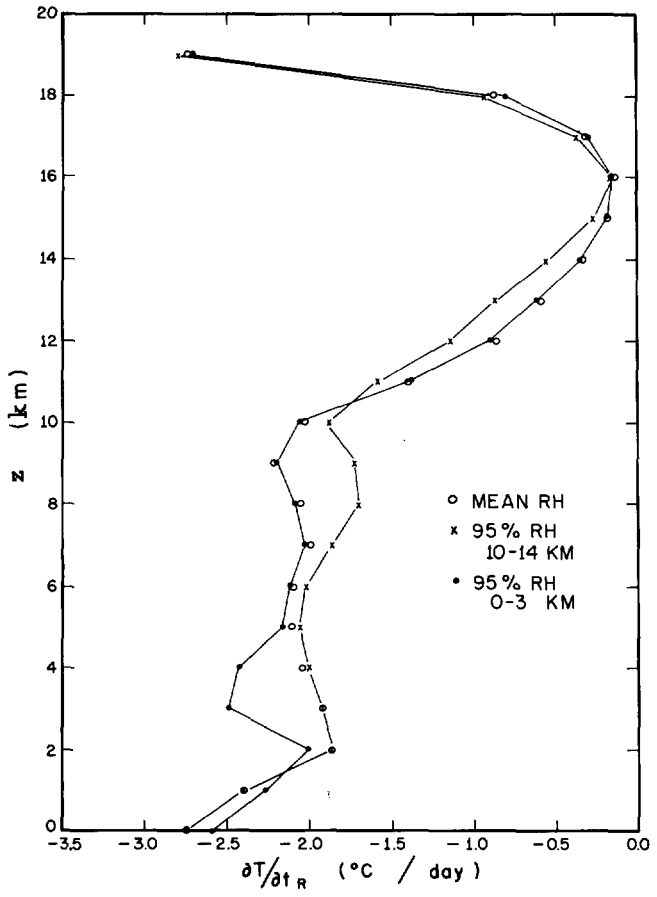

FIGURE 7.—Temperature change rates due to infrared flux divergence for various relative humidity distributions in the Tropics.

B. EXPERIMENTAL COOLING RATES

Height coordinates with 21 levels are utilized to provide high resolution ($\Delta z = 1$ km) for investigating the effects of different moisture distributions. In experiments with a resolution of 2 km, the mean cooling profiles are virtually unchanged. Thus, the vertical resolution needed to describe the essential features of cooling in a clear atmosphere is considerably less than 1 km. The vertical integrals are evaluated by the trapezoidal rule, and z_1 is assumed to be 20 km.

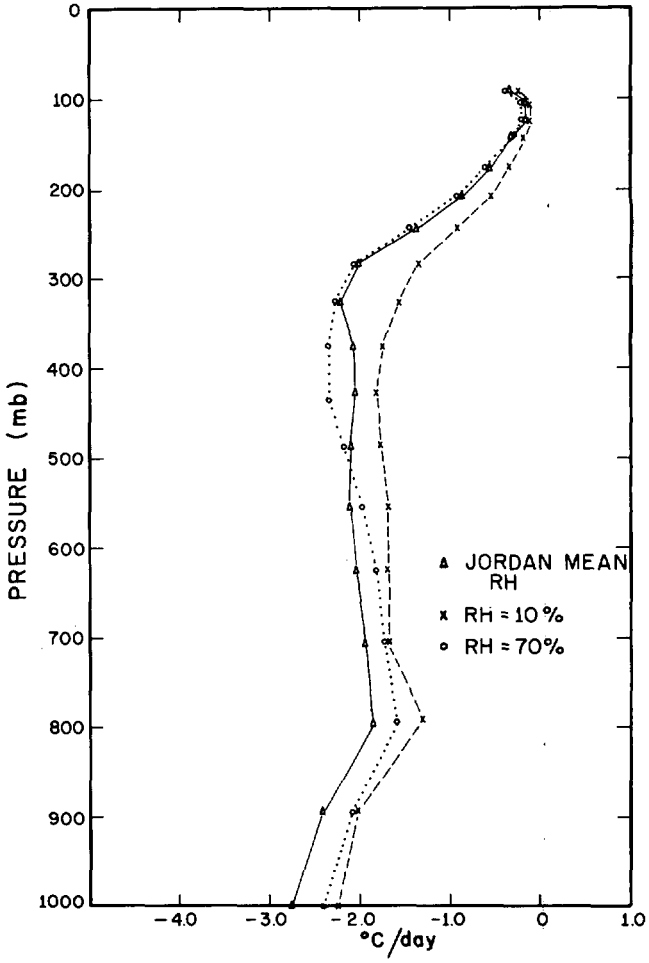

FIGURE 8.—Temperature change rates due to infrared flux divergence for various relative humidity distributions in the Tropics.

Figure 6 shows the upward, downward, and net fluxes from Jordan's (1958) mean hurricane sounding and the corresponding cooling rates caused by water vapor and carbon dioxide. The cooling effect from CO_2 is negligible compared to that from H_2O. A nearly constant cooling rate of 2°C/day occurs from the surface to 10 km. From 10 km to the tropopause, the cooling rate decreases, reaching a minimum of 0.1°/day near 16 km. Large cooling rates occur above the tropopause.

The next series of experiments is designed to investigate the dependency of the infrared cooling rates on the moisture distribution. The first two comparisons show the effect of nearly saturated layers, one close to the surface and the other high in the troposphere. Figure 7 shows the cooling profile that results from a 95-percent relative humidity in the layer from the surface to 3 km and another profile that results from a 95-percent relative humidity in the layer between 10 and 14 km. For the other layers, the temperature and moisture distributions are those of the mean hurricane sounding. Cooling is slightly increased above and decreased below the moist layers. Figure 8 shows the cooling rates that result from the mean hurricane season temperature sounding and two relative humidity profiles of 70 and 10 percent. Differences are again

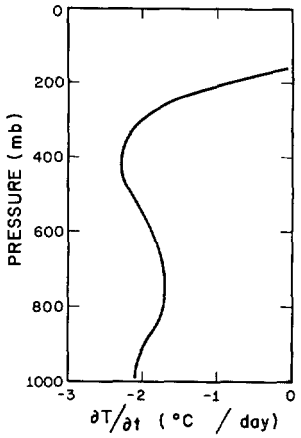

FIGURE 9.—Rate of temperature change due to infrared flux divergence used in the hurricane cooling experiment.

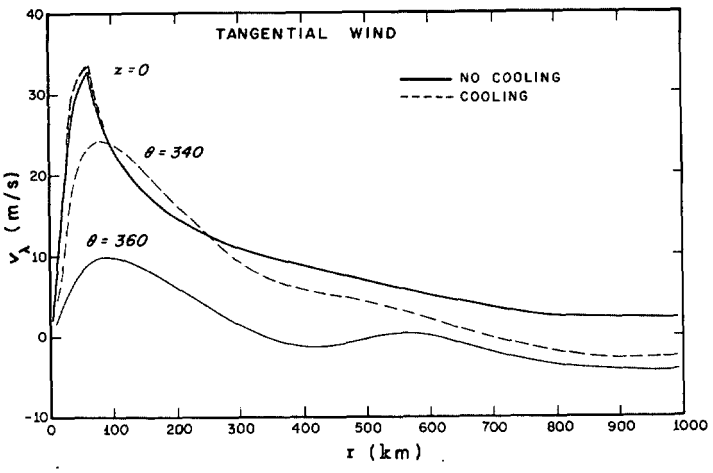

FIGURE 10.—Tangential wind profiles in experiment 11 (paper I) and experiment 6.

small with slightly lower cooling rates occurring in the drier air.

The relatively small dependency of the cooling rate on the moisture distributions justifies using the mean cooling rate in the hurricane model. Because the temperature in the hurricane environment is slowly varying, it is permissible to use the same cooling rate for several hours in numerical models of hurricanes. By such an approximation, the added storage and computational time are negligible. In this hurricane radiation experiment, the representative mean cooling profile (fig. 9) is nearly constant at 2°C/day below 400 mb and decreases to 0°C/day from 400 to 140 mb. It should be noted that the effect of clouds on infrared cooling is large; hence, this rate is valid only in the cloud-free region of the hurricane environment.

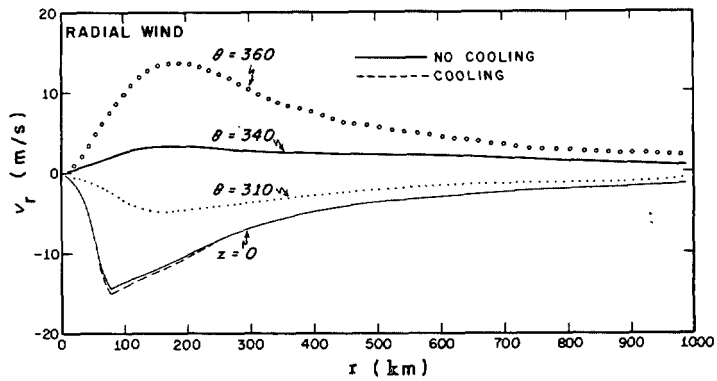

FIGURE 11.—Radial wind profiles in experiment 11 (paper I) and experiment 6.

C. RADIATIVE COOLING BEYOND 300 KILOMETERS, EXPERIMENT 6

Experiment 6 utilizes a 1000-km domain to study the effect of a uniform horizontal cooling from 300 km (assumed to be the edge of the cloud cover) to 1000 km. The control (no cooling) experiment is described in paper I as experiment 11.

Momentum and temperature structures. Figures 10, 11, and 12 show the tangential and radial wind profiles and the thermal structure for the cooling and noncooling experiments. The cooling results in an increase of 1.5 m/s in maximum tangential wind and an increase of 1 m/s in maximum inflow. As expected, the temperatures beyond 300 km are lower in experiment 6. A somewhat surprising result, however, is the cooling in the core of the storm, which is nearly as great as that in the outer regions. This cooling is apparently due to horizontal advection and mixing.

Energy budget. The difference in temperature structure (fig. 12) indicates that the radiative sink of energy is considerable. The total cooling of 3.4×10^{14} W is about a third of the total heating of 11.0×10^{14} W and confirms that the radiative heat loss is the same order of magnitude as the latent heat gain on the scale of 1000 km.

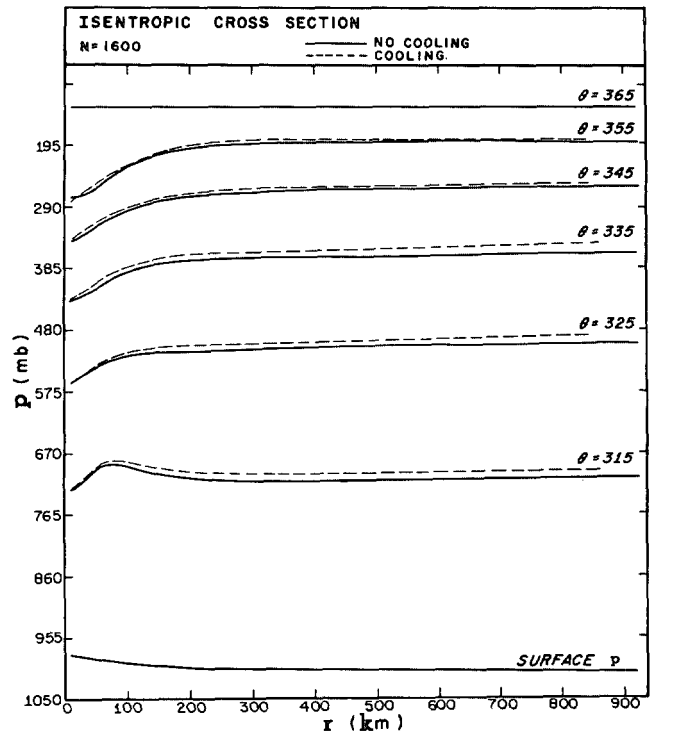

FIGURE 12.—Isentropic cross section for experiment 11 (paper I) and experiment 6.

The generation of available potential energy by the cooling is 0.2×10^{14} W or about 1.5 percent of the total generation. This is considerably less than the 17 percent estimated by Anthes and Johnson (1968). The difference is related to differences in temperature structures between hurricane Hilda and experiment 6. The Hilda environment contained greater large-scale baroclinicity beyond 500 km, resulting in larger negative efficiency factors. Thus cooling at 1000 km in the Hilda environment generates more available potential energy than in experiment 6. Another factor is the infrared emission in the region of positive efficiency factors. In Hilda, cooling was computed from 500 to 1000 km, a region of mostly negative efficiency factors. In experiment 6, cooling occurs from 300 to 1000 km. Because the 300- to 500-km region consists of positive efficiency factors, the infrared generation of available energy is negative in this region.

The total energy budget is summarized in table 1. Although the percentage of generation by radiation is less than 2 percent, the total generation is about 6 percent higher in the cooling experiment. Thus the slightly increased baroclinicity in the cooling experiment results in an increase in the generation by the latent heating.

Although the increase in maximum wind speed in the infrared experiment is only 1.5 m/s, the total cooling represents a significant energy sink. The infrared generation of available energy is considerably less than an earlier diagnostic estimate. Even though the cooling has a small effect on the dynamics of a mature storm in near-steady state, the possibility remains that it may play a more significant role in the earlier stages of tropical storm development. Because the formative stages frequently span several days, the cumulative effect of differential cooling between clear and cloudy regions may be significant. The gradual increase in baroclinicity could enhance the convective heating by accelerating the slow meridional circulation.

6. SUMMARY

This paper summarizes some additional experiments with an axisymmetric hurricane model in isentropic coordinates. A variable horizontal eddy viscosity coefficient of the type used by Smagorinsky et al. (1965) is used in these experiments. The results using variable exchange coefficients are similar to the previous results with constant coefficients.

Two additional latent heating functions are studied. Heating defined by a rainfall maximum of 100 cm/day near the center is sufficient to drive a moderate hurricane. A heating distribution with a secondary maximum at 200 km increases the radial extent of the storm but has a small effect on the maximum wind near the center.

Radiational cooling in the clear air is calculated for several moisture distributions in the Tropics using Sasamori's (1968) model. Infrared cooling beyond 300 km causes a 1.5 m/s increase in maximum wind speed and a 6-percent increase in the generation of available potential energy. The total heat loss by radiation on a scale of 1000 km is about one-half the total heat gain.

ACKNOWLEDGMENTS

The author wishes to thank Drs. Donald R. Johnson and Stanley L. Rosenthal for their helpful suggestions throughout this research. Mrs. Mary Jane Clarke typed the manuscript, and Mr. Robert Carrodus and staff prepared the figures.

REFERENCES

Anthes, Richard A., "A Numerical Model of the Slowly Varying Tropical Cyclone in Isentropic Coordinates," *Monthly Weather Review*, Vol. 99, No. 8, Aug. **1971**, pp. 617–635.

Anthes, Richard A., and Johnson, Donald R., "Generation of Available Potential Energy in Hurricane Hilda (1964)," *Monthly Weather Review*, Vol. 96, No. 5, May **1968**, pp. 291–302.

Gentry, R. Cecil, "A Study of Hurricane Rainbands," *National Hurricane Research Project Report* No. 69, U.S. Department of Commerce, Weather Bureau, Miami, Fla., Mar. **1964**, 85 pp.

Jordan, Charles L., "Mean Soundings for the West Indies Area," *Journal of Meteorology*, Vol. 15, No. 1, Feb. **1958**, pp. 91–97.

Koteswaram, P., "On the Structure of Hurricanes in the Upper Troposphere and Lower Stratosphere," *Monthly Weather Review*, Vol. 95, No. 8, Aug. **1967**, pp. 541–564.

Leith, Cecil E., "Two Dimensional Eddy Viscosity Coefficients," *Proceedings of the WMO/IUGG Symposium on Numerical Weather Prediction, Tokyo, Japan, November 26–December 4, 1968*, Japan Meteorological Agency, Tokyo, Mar. **1969**, pp. I–41—I–44.

Matsuno, Taroh, "Numerical Integrations of the Primitive Equations by a Simulated Backward Difference Method," *Journal of the Meteorological Society of Japan*, Ser. 2, Vol. 44, No. 1, Tokyo, Feb. **1966**, pp. 76–84.

Ooyama, Katsuyuki, "Numerical Simulation of the Life-Cycle of Tropical Cyclones," *Journal of the Atmospheric Sciences*, Vol. 26, No. 1, Jan. **1969**, pp. 3–40.

Orville, Harold D., "Ambient Wind Effects on the Initiation and Development of Cumulus Clouds Over Mountains," *Journal of the Atmospheric Sciences*, Vol. 25, No. 3, May **1968**, pp. 385–403.

Phillips, Norman A., "An Example of Non-Linear Computational Instability," *The Atmosphere and the Sea in Motion*, Rockefeller Institute Press, New York, N.Y., **1959**, pp. 501–504.

Riehl, Herbert, and Malkus, Joanne S., "Some Aspects of Hurricane Daisy, 1958," *Tellus*, Vol. 13, No. 2, Stockholm, Sweden, May **1961**, pp. 181–213.

Rosenthal, Stanley L., "A Circularly Symmetric Primitive Equation Model of Tropical Cyclone Development Containing an Explicit Water Vapor Cycle," *Monthly Weather Review*, Vol. 98, No. 9, Sept. **1970**. pp. 643–663.

Sasamori, Takashi, "The Radiative Cooling Calculation for Application to General Circulation Experiments," *Journal of Applied Meteorology*, Vol. 7, No. 5, Oct. **1968**, pp. 721–729.

Smagorinsky, Joseph, Manabe, Syukuro, and Holloway, J. Leith, Jr., "Numerical Results From a Nine-Level General Circulation Model of the Atmosphere," *Monthly Weather Review*, Vol. 93, No. 12, Dec. **1965**, pp. 727–768.

Staff, National Hurricane Research Laboratory, *PROJECT STORMFURY, ANNUAL REPORT, 1968*, Miami, Fla., **1969**, 40 pp.

[*Received August 19, 1970; revised January 22, 1971*]